AN EVALUATION OF VACUUM DEPOSITED METAL-INSULATOR-PIEZOELECTRIC SEMICONDUCTOR (MIPS) ELECTROMECHANICAL TRANSDUCERS

by

J. R. Fiebiger and R. S. Muller

Memorandum No. ERL-M166

21 June 1966

ELECTRONICS RESEARCH LABORATORY

College of Engineering
University of California, Berkeley
94720

Manuscript submitted: 18 May 1966

The research reported herein was supported wholly by the Joint Services Electronics Program (U. S. Army, U. S. Navy, and U. S. Air Force) under Grant AF-AFOSR-139-66.

ABSTRACT

The theory underlying the operation of metal-insulator-piezoelectric (MIPS) electromechanical transducers is verified experimentally for time-varying loads on devices made from CdS piezoelectric film materials. Experimental transducers exhibit sensitivities of the same order as those observed under static loading within times shorter than one microsecond after the application of mechanical stress. The frequency limitations for the transducer appear to be determined by the electrical properties of the MOS structure. The MIPS effect is demonstrated experimentally in CdSe transducers. Transducers fabricated on a flexible polyimide film are described, and a microphone embodying this construction is discussed.

TABLE OF CONTENTS

LIST OF FIGURES

I. INTRODUCTION

The use of the piezoelectric effect in an insulated-gate, field-effect, transistor structure fabricated of a piezoelectric semiconductor is described by Muller and Conragan.[1,2] Conragan[3] performed extensive experiments on CdS MIPS transducers using static loading conditions to prove the basic theoretical model for the stress sensitivity. This report is concerned with further evaluation of vacuum-deposited MIPS transducers, particularly emphasizing dynamic measurements on the devices.

The MIPS transducers used for these studies were thin-film, cadmium sulfide (CdS) and cadmium selenide (CdSe) transistors which were fabricated in the Electronics Research Laboratory. The fabrication procedures and device geometry are described in more detail in a separate section.

The static electromechanical transducer tests, as described by Conragan,[3] were carried out on all devices fabricated. The results of these tests were in excellent agreement with the theory. In the study of the transient performance of CdS MIPS transducers, no limiting response time longer than the time constant associated with transconductance cut-off of the MOS transistor structure was found. Responses to strains were clearly discernible less than a microsecond after impact loading.

Typical MIPS devices have been shown theoretically to be approximately three hundred times more sensitive than high-quality, commercial, semiconductor strain gages.[1] This theoretical value agrees with experimental comparisons between the measured performances of MIPS devices and commercial gages.

A MIPS transducer evaporated onto a one-mil thick membrane of "Kapton," a polyimide film described in Section II, was used to make a microphone.[4] Although the mounting scheme was relatively crude, it was a simple matter to deliver a 10 mV signal to a 10 KΩ load when the device was activated by a normal speaking voice.

The paper is organized in the following manner. First, a brief discussion of the piezoelectric properties of the materials is given; then a theoretical analysis of the stress effect in a MIPS transducer is presented. Next, the device fabrication procedures and geometry are described. This is followed by a summary of the equations for the strain applied to the MIPS device. A comparison is then made of experimental and theoretical calculations. Following this, the implications of this study are enumerated and discussed.

II. THEORETICAL CONSIDERATIONS

A. Material Properties

The transducer properties are dependent on the piezoelectric nature of deposited thin-films of CdS and CdSe. Therefore, it is of value to begin with an enumeration of the mechanisms underlying piezoelectricity in the films.

Both CdS and CdSe crystallize in two polymorphic forms, the cubic zinc blende structure (sphalerite) and the hexagonal structure (wurtzite). Both crystal structures can be built up from cadmium and sulfur or selenium atoms bonding mutually with tetrahedral s, p-hybrid bonds of partly ionic character. Thus, each atomic type can be characterized by a tetrahedral configuration of dipole moments as shown in Fig. 1. As is evident in Fig. 1, when an atom of cadmium and sulfur or selenium are joined, the dipole moment of the two partners may be arranged in either an eclipsed or staggered configuration if the structure is viewed along the c-axis. Thus, the two structures of CdS and CdSe result, formed by diatomic molecules oriented with their axes parallel to the c-direction and crystallized either in the staggered (sphalerite) or eclipsed (wurtzite) orientation of their moments, as shown in Fig. 1. The c-direction shown in Fig. 1 corresponds to the [111] direction in the cubic zinc blende (sphalerite) structure and to the c-axis of the hexagonal wurtzite structure.

To understand the piezoelectric effect in these crystals, recall that the bonding of II-Vi compounds has a substantial ionic content, so that each diatomic pair has a net dipole moment. With this in mind, consider the effect of a stress on the two structures discussed above.

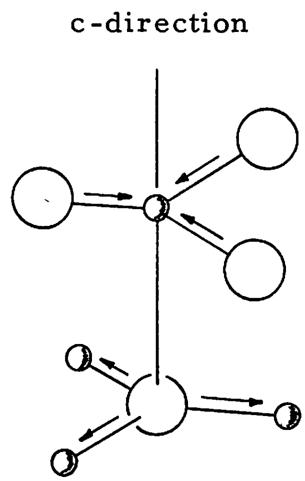

CdS and CdSe tetrahedral arrangements.

Cd

S or Se

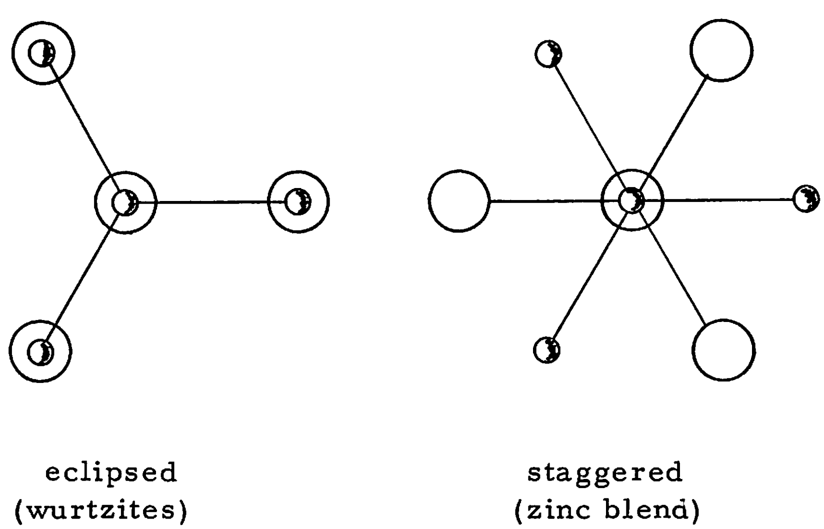

Fig. 1. Possible orientation of CdS and CdSe in tetrahedral bonding.

Stress in the c-direction tends to compress the c-directed dipoles axially but acts to rotate the three remaining dipoles. Dipole rotation is more easily accomplished and its effect dominates the piezoelectric behavior in the crystals. Rotation of the nonaxial dipoles reduces the c-directed components of their moments and causes a net polarization.

X-ray analysis of the deposited CdS films made in this laboratory shows that the CdS films are approximately 90% wurtizite structure with the c-axis normal to the substrate.[5] Preliminary results of x-ray studies on the CdSe films (Appendix) indicate that the films tend to be composed of either wurtzite structure with the c-axis normal to the substrate surface or of the zinc blende structure with the [111] direction normal to the substrate. For films so oriented the [e] and [s] matrices reduce to[6]

$$[S] = \begin{bmatrix} S_{11} \\ S_{22} \\ S_{33} \\ S_4 \\ S_5 \\ S_6 \end{bmatrix}$$

where $S_4 = 2S_{21}$,

$S_5 = 2S_{13}$,

$S_6 = 2S_{12}$

and

$$[e] = \begin{bmatrix} 0 & 0 & 0 & 0 & e_{15} & 0 \\ 0 & 0 & 0 & e_{15} & 0 & 0 \\ e_{31} & e_{31} & e_{33} & 0 & 0 & 0 \end{bmatrix}$$

The coordinate system that is used is shown in Fig. 2 where the x_3 direction is chosen normal to the plane of the substrate.

For the manner in which the strains are applied in all experiments to be described, S_{33} can be expected to be very small. The only stress leading to a non-zero S_{33} would result from oxide tension. Since the oxide is approximately 400 Å thick, S_{33} is expected to be negligible. For all experiments conducted, the substrate was stressed in a manner such that either S_{11} or S_{22} is zero, but not both simultaneously.

B. Transducer Theory

The piezoelectric properties of the crystalline films discussed in the last section are combined with their semiconducting properties to make a MIPS transducer. The transducer relies on the characteristics of insulated gate field-effect transistors. If the semiconductor region of a metal-oxide semiconductor (MOS) transistor is piezoelectric, stress applied to the layer will induce a charge density at the surface of the semiconducting layer. This piezoelectrically-induced charge will

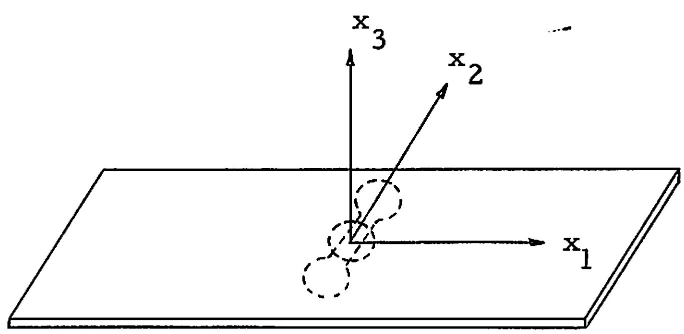

Fig. 2. Orientation of axes used in analysis of MIPS effect.

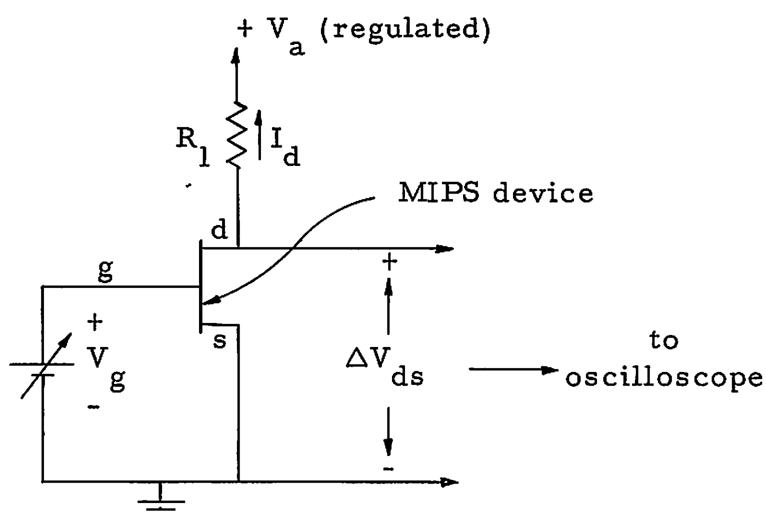

Fig. 3. MIPS device bias and detection circuit.

change the gate-offset voltage V_o. The change in $V_o (\Delta V_o)$ is given by the equation:[1]

$$\Delta V_o = [e] [S] \cdot [n]/C'_g \tag{1}$$

where C'_g = effective gate channel capacitance/unit area,

[S] = applied strain matrix,

[n] = unit normal to the surface matrix, and

[e] = piezoelectric coefficient matrix for the semiconducting material.

Under the conditions described in the previous section, many of the matrix elements vanish so that Eq. (1) becomes:

$$\Delta V_o = e_{31} S_s / C'_g , \tag{2}$$

or

$$S_s = \Delta V_o \, C'_g / e_{31} , \tag{3}$$

where S_s is the strain at the surface of the substrate, S_{11} or S_{22}.

In the pinch-off region of operation, $V_d > (V_g - V_o)$, the drain current I_d is given by[7]

$$I_d = I_{do}\left(V_g - V_o\right)^n \approx \mu \, \epsilon_i \, W\left(2t_i \, L\right)^{-1} \left(V_g - V_o\right)^n , \tag{4}$$

where I_{do} = drain current at zero gate voltage,

μ = effective mobility of free carriers,

t_i = thickness of the insulator,

ϵ_i = permittivity of the insulator layer,

W = channel width,

L = channel length = source-drain electrode spacing,

V_d = drain-source voltage,

V_g = gate-source voltage,

V_o = gate-offset voltage of the device.

The exponent n is in the range of 2 to 3 for devices with constant mobility and for which the oxide thickness is appreciably greater than the channel depth.

If we let I_{ds} and ΔI_{ds} be the strained and strain-induced change in the quiescent value of drain current I_d, respectively, we have:

$$\begin{aligned} I_{ds} &= I_{do}\left[V_g - \left(V_o + \Delta V_o\right)\right]^n \\ &= I_{do}\left(V_g - V_o\right)^n \left[1 - \Delta V_o/\left(V_g - V_o\right)\right] \\ &= I_d\left[1 - \Delta V_o/\left(V_g - V_o\right)\right]^n , \end{aligned} \tag{5}$$

or

$$V_o = \left(V_g - V_o\right)\left[1 - \left(I_{ds}/I_d\right)^{1/n}\right]$$

$$= \left(V_g - V_o\right)\left[1 - \left(1 + \Delta I_{ds}/I_d\right)^{1/n}\right] \; . \qquad (6)$$

Therefore, we can solve for the surface strain S_s by using Eq. (3) and (6).

$$S_s = \left(C_g'/e_{31}\right)\left(V_g - V_o\right)\left[1 - \left(1 + \Delta I_{ds}/I_d\right)^{1/n}\right] \; . \qquad (7)$$

Useful expressions for the parameters V_o and n may be derived in the following manner:

$$g_m = \left.\frac{\Delta I_d}{\Delta V_g}\right|_{\Delta V_d = 0} = n I_{do}\left(V_g - V_o\right)^{n-1} \; , \qquad (8)$$

so

$$I_d/g_m = n^{-1}\left(V_g - V_o\right) \; . \qquad (9)$$

Thus, if experimental values of I_d/g_m are plotted versus V_g, the zero intercept on the V_g axis will indicate V_o, and the slope will yield $1/n$.

If $|\Delta I_{ds}/I_d|$ is less than 0.2, a Maclaurin expansion of Eq. (7), which is valid to within 3% of the exact value, is given by:

$$S_s = -n^{-1}\left(V_g - V_o\right)\left(\Delta I_{ds}/I_d\right)\left(C_g'/e_{31}\right) . \tag{10}$$

The equation for $\Delta I_{ds}/I_d$ is readily found from Eq. (5) to be:

$$\Delta I_{ds}/I_d = \left(I_{ds} - I_d\right)/I_d$$

$$= \left[1 - \Delta V_o/\left(V_g - V_o\right)\right]^n - 1 . \tag{11}$$

From Eq. (11), it is clear that for a given strain, the percentage change in I_d (i.e., $\Delta I_{ds}/I_d$) increases as the bias current I_d decreases, because $\left(V_g - V_o\right)$ decreases with I_d. It is also clear, however, that the change in the absolute value of I_d (i.e., ΔI_{ds}) for a given strain increases with quiescent operating current I_d. Hence, if it is desirable to maintain a linear relation between the applied strain and the strain-induced change in drain current ΔI_{ds}, the quiescent current I_d must be chosen to be large enough so that $\left|\Delta I_{ds}/I_d\right|_{max} < 0.2$.

Equations (9) and (10) may be combined to yield

$$S_s = -\frac{\Delta I_{ds}}{g_m}\frac{C_g'}{e_{31}} \tag{12}$$

for the surface strain. Equation (12) is simple to apply, and it is the form used in most of this report. If $\left|\Delta I_{ds}/I_d\right|$ is much greater than 0.2, the more general relation given by Eq. (7) must be used.

The effective gate-capacitance per unit area C'_g for a particular MIPS device is determined from a simple capacitance bridge measurement and the dimensions of the active region or channel. The piezoelectric coefficient e_{31} for single crystal wurtzite structure CdS and CdSe is known.[8] After a quiescent drain current I_d is chosen, the corresponding transconductance g_m can easily be found by varying the gate-voltage V_g slightly and then using measured increments of V_d and I_d in the approximate relation:

$$g_m = \left.\frac{\Delta I_d}{\Delta V_g}\right|_{\Delta V_d = 0} . \tag{13}$$

After C'_g and g_m are determined, any strain is readily calculated by measuring the corresponding ΔI_{ds} and applying Eq. (12).

In some cases the strain-induced change in drain current, ΔI_{ds}, may be small enough so that it is difficult to measure directly. Since a MIPS device has output characteristics closely approximating those of a current source, i.e., a high output resistance, a large load resistance can be connected in series with the drain as shown in Fig. 3, and ΔV_{ds} for constant applied voltage V_a can be measured. Alternatively, a bridge circuit may be used to determine ΔI_{ds}.

The method used to measure ΔI_{ds} for this report is the first described in the previous paragraph and is indicated in Fig. 3. From the circuit of Fig. 3,

$$\Delta V_{ds} = -\Delta I_{ds} R_1 ,$$

thus, Eq. (13) becomes

$$S_s = \frac{\Delta V_{ds}}{g_m R_1} \frac{C'_g}{e_{31}} . \tag{14}$$

It should be noted that for the circuit of Fig. 3,

$$g_m R_1 = \left. \frac{\Delta V_a}{\Delta V_g} \right|_{\Delta V_d = 0} \tag{15}$$

The strain-induced change in source-to-drain voltage ΔV_{ds} may be made very large by increasing the load resistance R_1 provided that ΔV_{ds} is greater than the noise voltage across R_1. The voltage ΔV_{ds} must not be so large that the device comes out of the pinch-off region of operation $\left[\text{i.e.,}\ V_{ds} = \left(V_d - \Delta V_{ds}\right) \leq \left(V_g - V_o\right)\right]$ or the equations for the surface strain S_s will not be valid. Since typical quiescent source-drain voltages V_d are approximately 5 volts for pinch-off voltages less than 1 volt, values of ΔV_{ds} in the range of 3 volts may easily be attained.

If the load resistance approaches the output resistance r_o of the MIPS device, then $\Delta V_{ds}/R'\big|_{V_a=\text{const.}}$ (where $R'^{-1} = R_l^{-1} + r_o^{-1}$) may be used for ΔI_{ds} in Eq. (12).

For quiescent drain currents I_d comparable to the source-drain leakage current that flows at pinch-off, the equations derived for surface strain S_s will be in error since this leakage component was not considered in the theory used here. The leakage current is in general very small (0.1 μa was typical for devices used) and can be neglected for reasonable values of quiescent drain current I_d.

The time required for the strain-induced charge density to appear at the surface of the piezoelectric semiconductor or the time for the strain-induced change in built-in potential ΔV_o to be produced after the application of a strain in the dielectric relaxation time of the semiconductor. The dielectric relaxation time for CdS and CdSe evaporated films suitable for use in fabricating MOS transistors is less than approximately 10^{-10} seconds, and hence is negligible compared to other delays which will be discussed. Since the MIPS transducer can be made as thin as one micron, delays associated with strain propagation to the active region of the tranducer can be designed to be negligible for frequencies less than approximately one GHz. Thus, the appropriate response time which would characterize the MIPS device is the response time of the MOS transistor structure. Therefore, the previously derived equations for surface strain S_s [Eqs. (7), (10),

(12) and (14)] will be valid at times large when compared with the time required for the MOS transistor structure to respond to a step function of gate voltage. If ΔI_{ds} is measured directly by using a low impedance, high frequency detector, the ultimate response time of the transducer t_r,[9,10] is the rise time associated with the input capacitance and transconductance of the device,

$$t_r = C_{in}/g_m \; . \tag{17}$$

III. SAMPLE FABRICATION

The MIPS transducers used for these studies were of the coplanar-type (Fig. 4) constructed entirely by vacuum deposition techniques. Both cadmium sulfide and cadmium selenide were used for the semiconductor layers.

A detailed description of the process and apparatus used for constructing CdS devices is presented by Conragan.[3] The apparatus used to make CdSe devices is the same. The only process changes involve replacing CdS with ultra-high purity CdSe and using slightly reduced source and substrate temperatures. The CdS used for deposition was Eagle Picher's ultra-high purity grade polycrystalline

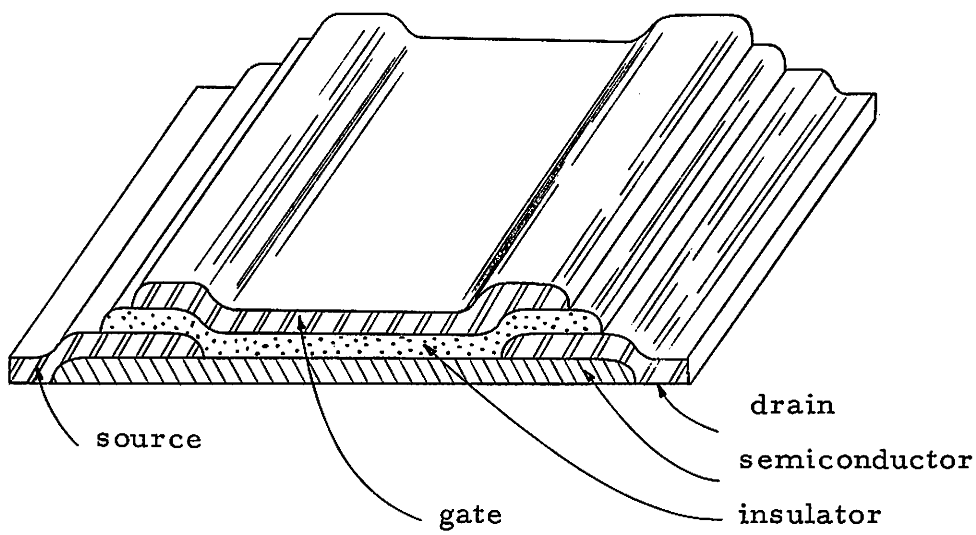

Fig. 4. Coplanar-Type MIPS transistor.

material; the CdSe source was Harshaw's "random cutting" crystalline material.*

The procedure used to make these coplanar-type devices is described briefly below. In a vacuum of 10^{-6} Torr, the CdSe (CdS) layer was deposited at a temperature of 720° C (760° C) onto the substrate heated to 130° C (180° C). This was followed by deposition of the aluminum source-drain electrodes and then the SiO insulating layer. Finally, the gate electrode was deposited.

The dimensions of the piezoelectrically active region (channel) for the devices used were 0.001×0.100 in. The thickness of the semiconductor layer was on the order of 1 micron and the oxide thickness was roughly 400 angstroms.

The substrate materials employed were standard microscope slides, Corning 7059 substrate glass, and "Kapton."** There was no noticeable difference between devices made with the three substrate materials. The adherence of both CdS and CdSe MIPS devices to all three substrates were sufficient to pass the "Scotch-tape test."

Only the substrate cleaning process needed to be changed from the procedure used by Conragan to make MIPS transistors on a

---

* Trade name.

** Trade mark for a polyimide film developed by E. I. du Pont de Nemours, Inc., du Pont Chestnut Run Laboratories, Wilmington, Delaware.

Kapton substrate. Sheets of Kapton 1 mil thick were fastened to glass slides for ease of handling. Then the Kapton substrates were swabbed and rinsed with methyl alcohol, blown dry with nitrogen, and immediately placed in the vacuum system for deposition of the MIPS device.

A photograph of one of the CdSe devices on a Kapton substrate is shown in Fig. 5(a). Figure 5(b) is a Polaroid photograph of the MIPS transistor characteristics, displayed on a Tektronix Type 575 transistor curve tracer, for the device of Fig. 5(a).

IV. COMPARISON OF EXPERIMENTAL AND THEORETICAL RESULTS

In this section, experimental data obtained by stressing CdS and CdSe MIPS transducers are presented and compared with the results of calculations based on beam theory. The experimental procedures and measurements are described first for each mounting and loading of the MIPS device substrate. This description is followed by calculations of the applied strain based on beam theory. Next, the measured data from representative devices are given and the corresponding values of strain are calculated from the theory presented in Sec. II. Finally, the results are compared and conclusions are drawn.

The gate-electrode capacitance of all of the MIPS devices used for this project was measured with a General Radio Company type

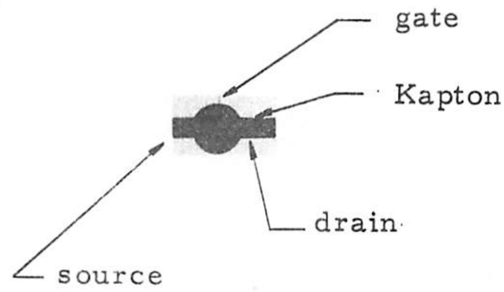

(a) an actual size photograph

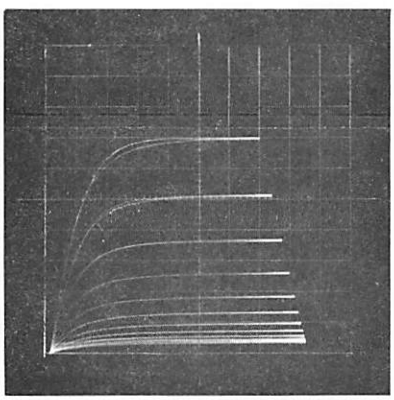

horizontal = V_d = 0.5 V/div
vertical = I_d = 0.2 ma/div
V_g = 0.1 V/div
V_g(max) = 1.0 V

(b) transistor characteristics of the devices shown in (a)

Fig. 5. CdSe MIPS transducer made on a "Kapton" substrate.

1608-A impedance bridge. The capacitance was measured at a frequency of 1 kHz. In most devices, the gate electrode overlaps the source and drain electrodes. The amount of this overlap was measured optically. The measured value of gate capacitance was then adjusted to represent the active gate capacitance C_g. The effective gate capacitance per unit area C'_g is found by dividing C_g by the channel area. The dimensions of the channel for all devices was 0.001×0.100 in., as given in the Appendix.

Thus, these devices have a channel area of $6.25 \times 10^{-8}\ m^2$. The effective gate capacitance per unit area C'_g is believed to be accurate to within $\pm 10\%$.

A. Dynamic Response of CdS MIPS Transducers

Conragan[3] obtained convincing experimental proof of the MIPS theory for static load conditions. In order to study the response to dynamic stress, one experiment employed an ultrasonic drill vibrating at a frequency of 19.5 kHz to strain glass-mounted MIPS transducers. The substrate was strained in the manner shown in Fig. 6. The applied strain for this method of stressing the MIPS device can be found in texts dealing with mechanics of solids[11] and is given by:

$$S_s(x, t) = \frac{48t_s\, d(t)}{L^3} \left[x - \frac{1}{4} L\right] \left\{1 + \left[\frac{48d(t)}{L^3} \left(x^2 - \frac{1}{2} Lx\right)\right]^2\right\}^{-3/2}, \quad (18)$$

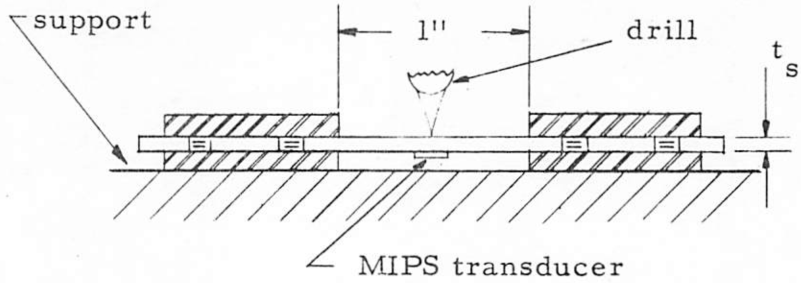

(a) loading

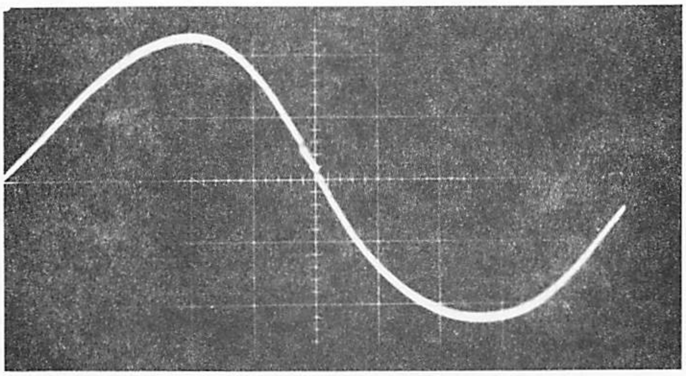

vertical = $\Delta V_{ds}(t)$ = 0.1 V/div

horizontal = 5 μs/div

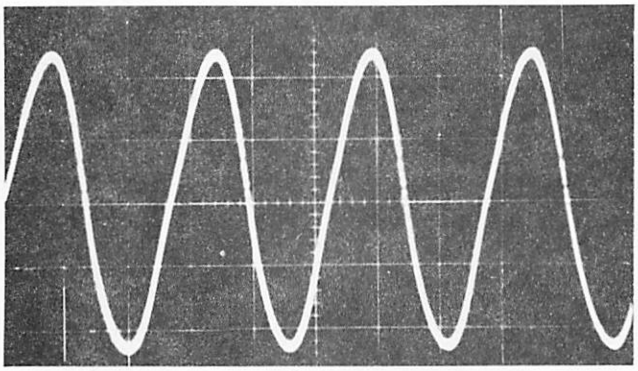

vertical = $\Delta V_{ds}(t)$ = 0.1 V/div

horizontal = 20 μs/div

(b) oscilloscope photographs of the strain induced change in source-drain voltage versus time.

Fig. 6. Ultrasonic drill experiment.

where t_s = thickness of substrate glass,

$d(t)$ = maximum displacement of substrate glass as a function of time.

For all MIPS transducers, t_s and L in Eq. (18) were 0.034 and 1.0 in., respectively. The maximum displacement d_{max} of the substrate is known to be between 0.1 and 1.0 mil from detailed measurements made on an ultrasonic drill with an identical resonant section and driving power. From Eq. (18) the maximum surface strain is found to be in the range of 0.5×10^{-4} to 5.0×10^{-4}.

The a.c. output voltage observed across the source to drain electrodes of a typical CdS device* is shown in the oscilloscope photographs of Fig. 6b. The output of this MIPS device is seen to be a nearly sinusoidal voltage with an amplitude of 0.44 volts at a frequency of 19.5 kHz. The biasing and detection circuit is the same as shown in Fig. 3 with $R_l = 50\ K\Omega$. Figure 7 shows a plot of I_d/g_m versus V_g, for the device of Fig. 6, constructed by varying the quiescent operating point and applying Eq. (15).

$$g_m = \frac{1}{R_l} \frac{\Delta V_a}{\Delta V_g}\bigg|_{\Delta V_d = 0} .$$

---

* The device used for all dynamic tests were constructed such that there was no gate overlap of the source and drain electrodes in order to improve the frequency response of the MIPS transistor.

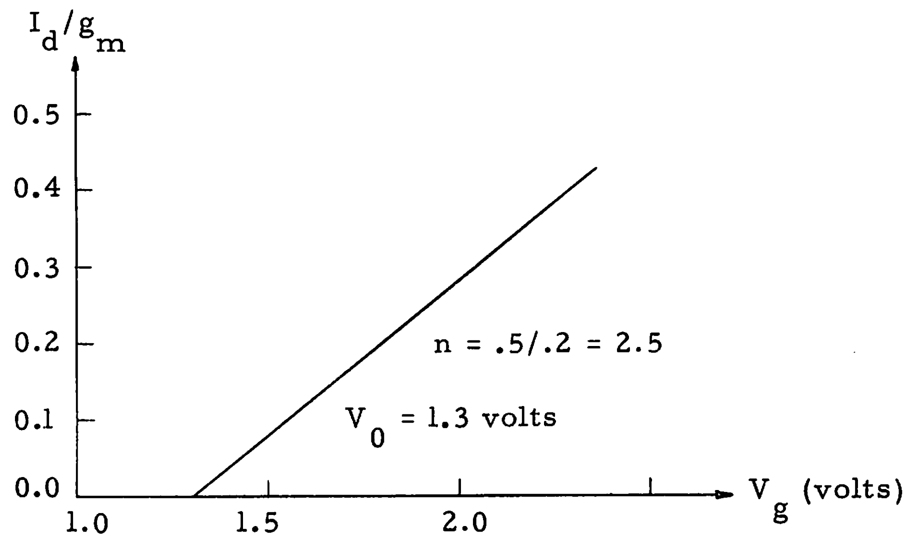

Fig. 7. Plot of I_d/g_m versus V_g for the MIPS device of Fig. 6.

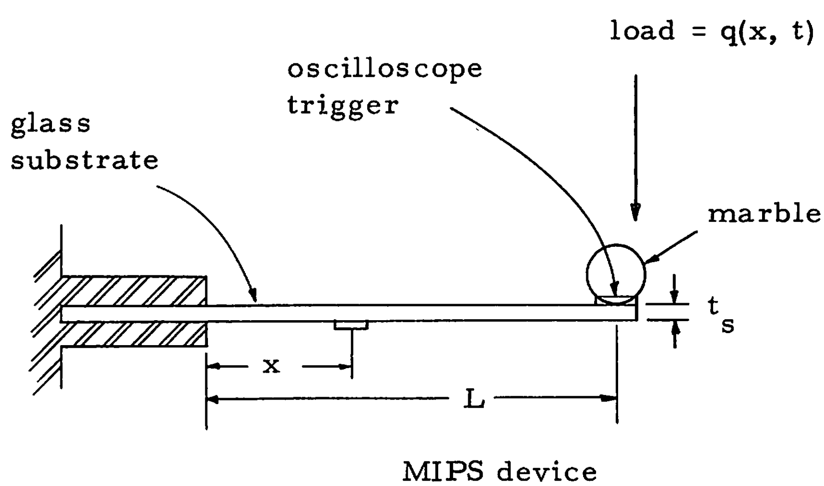

Load q(x, t) is produced by the marble impacting the free end of the cantilever-mounted MIPS device glass substrate

Fig. 8. Impact-loaded, cantilever-mounted MIPS device glass substrate.

From this plot, the values of the parameters n and V_o are found to be 2.5 and 1.3 volts, respectively. The measured gate capacitance was 116 pf. so $C'_g = (116 \times 10^{-12}) / (6.25 \times 10^{-8}) = 0.186$ fd./m^2. The quiescent operating point was $I_d = 100$ μa for $V_g = 2.2$ volts. For CdS, the piezoelectric coefficient $e_{31} = -0.244$ c/m^2. Upon substitution of the above data into Eq. (7) we have

$$S_{s(max)} = \frac{C'_g}{e_{31}} \left(V_g - V_o\right) \left[1 - \left(1 - \frac{\Delta V_{ds(max)}}{R_1 I_d}\right)^{1/n}\right]$$

$$= \frac{.186 \times 10^{-2}}{-.244} (.9) \left[1 - \left(1 + \frac{.44}{(50 \times 10^3)(10^{-4})}\right)^{.4}\right]$$

$$= 2.35 \times 10^{-4} .$$

Hence the value of peak strain calculated from MIPS theory is in the range found using beam theory. The results of this ultrasonic drill experiment are significant because they show that MIPS electromechanical transducers have a sensitivity equal to the static value at least to 20 kHz.

Transient response studies of CdS MIPS transducers were made by impacting the free end of cantilever-mounted, d.c. biased MIPS devices as shown in Fig. 8. The circuit of Fig. 3 with $R_1 = 10.65$ KΩ was used to bias the device. The rise time associated with the output where K' = constant for a particular quiescent operating point. Then, by MIPS theory the oscilloscope traces of Fig. 9 are proportional to the surface strain. Hence, the oscilloscope traces of Fig. 9 should be different from theoretical solutions for the applied surface strain $S_s(x, t)$ only in amplitude.

The surface strain can be obtained theoretically by solving the one-dimensional Bernoulli-Euler beam equation

$$\frac{\partial^2}{\partial x^2}\left[EI\,\frac{\partial^2 v}{\partial x^2}\right] + m\,\frac{\partial^2 v}{\partial t^2} = q(x, t) \; . \qquad (20)$$

In order to obtain values for S_s, one must solve Eq. (20) and use the solution to calculate:

$$S_s(x, t) = \frac{1}{2}\,t_s\,\frac{\partial^2}{\partial x^2}\,v(x, t) \; . \qquad (21)$$

Except for idealized (and nonphysically realizable) loading functions, this procedure is very difficult.

A complex method for solving the Bernoulli-Euler equation (Eq. (20)) for elastic beams that are impacted transversely with hard solid spheres has been developed by W. Goldsmith and K. E. Barnhard, Jr.[12] The theory incorporates a dynamic plastic force-indentation law and linear elastic boundary conditions. A method is also devised to

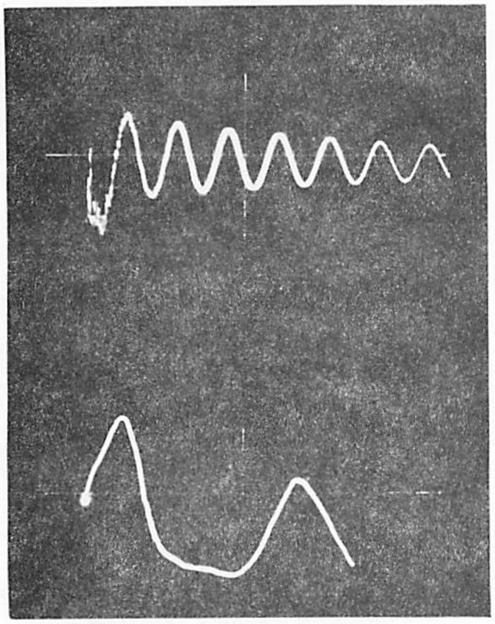

(a)
top - horizontal = 5 ms/div
bottom - horizontal = 20 μs/div

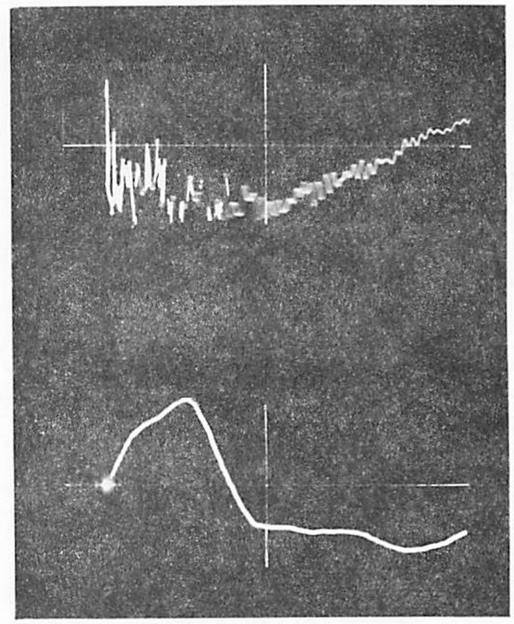

(b)
top - horizontal = 0.5 ms/div
bottom - horizontal = 10 μs/div

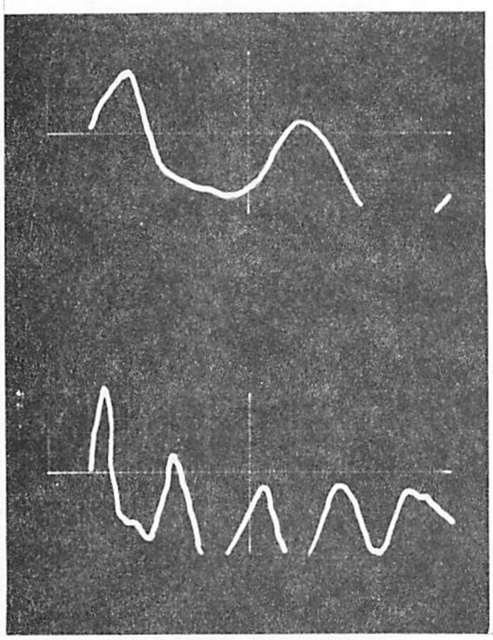

(c)
top - horizontal = 20 μs/div
bottom - horizontal = 50 μs/div

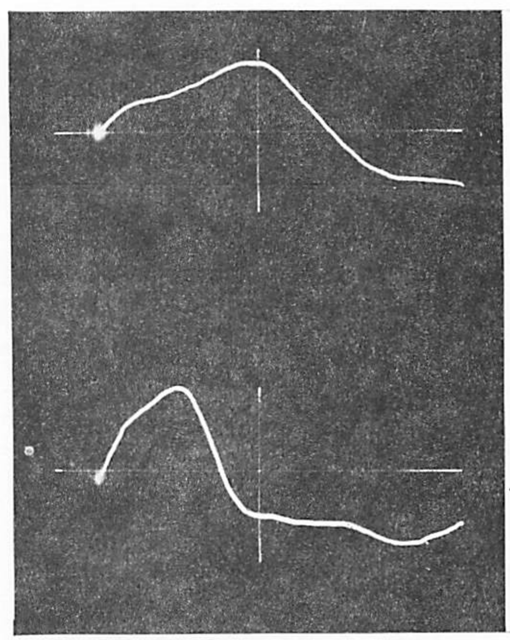

(d)
top - horizontal = 5 μs/div
bottom - horizontal = 10 μs/div

vertical = $\Delta V_{ds}(t)$ in 0.1 V/div for all photographs

Fig. 9. Response of MIPS device to mechanical impact load.

capacitance and resistance was prevented from affecting the response by decreasing the load resistance until the rise time of the MOS transistor to a step in gate voltage remained constant.

Oscilloscope traces of the strain-induced change in source-to-drain voltage, $\Delta V_{ds}(t)$, for a typical MIPS transducer are shown in Fig. 9. The trace was triggered by the marble contacting the glass substrate which supports the MIPS device.

No limiting response time longer than the time constant associated with the input capacitance and transconductance (Eq. 17) was found. Responses to strains less than a microsecond after impact were clearly discernible, as is evident in Fig. 9.

Figure 10 shows the response of the d.c. biased MIPS transistor, used to obtain Fig. 9, to a step in gate voltage. The rise time of the amplifier is seen to be approximately 2.0 μsec. The rise time of the first peak of the mechanically induced $\Delta V_{ds}(t)$ is seen from Fig. 9 to be about 20 μsec. Hence it appears that the limiting response to applied strain is in the mechanical system.

The quiescent operating current for all MIPS transient response studies was high enough that $\Delta V_d(t)_{max}/R_l I_d < 0.2$. Therefore, from MIPS theory the surface strain is given by Eq. (14).

$$S_s(t) = \frac{\Delta V_{ds}(t)}{g_m R_l} \frac{C'_g}{e_{31}} = K' \Delta V_{ds}(t) \tag{19}$$

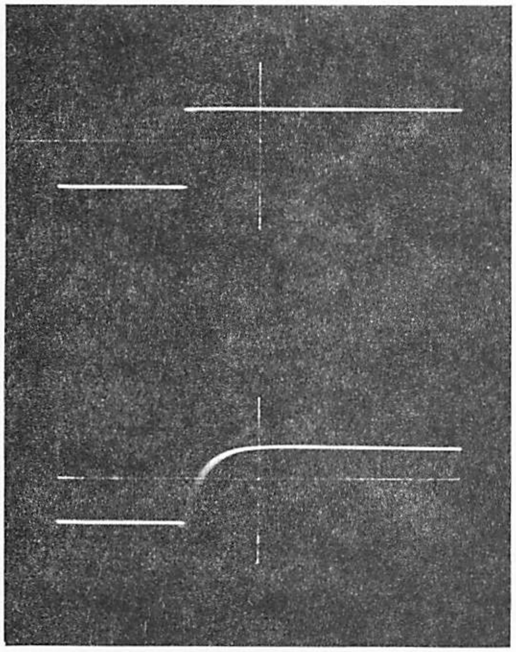

(top)

vertical = 0.1 V/div
horizontal = 2 μs/div

(bottom)

vertical = 0.2 V/div
horizontal = 2 μs/div

top = step in gate voltage applied to the MIPS device
bottom - ΔV_d response of the MIPS device to the gate step

Fig. 10. Response of d.c. biased CdS MIPS device to a step in gate voltage.

account for the effect of an infinite number of bending modes in the solution. When this method for solving the Bernoulli-Euler equation is used, the force-time relation is first found and then the corresponding stress or strain is obtained. The theory yields good agreement with experimental measurements for times prior to the occurrence of the first peak in the curve representing strain vs time. Barnhart and Goldsmith observed that the initial peak strain frequently represents the maximum or near maximum stress condition during the entire beam response.[12] This result is in agreement with strain vs time curves such as Fig. 9, obtained from the MIPS device.

A study of the results obtained by Goldsmith and Norris[13] for surface stress as a function of time for cantilever mounted beams impacted in the manner shown in Fig. 8 led to the conclusion that the beam surface strain given by the MIPS transducer in Fig. 9 is very reasonable.

Attempts to reproduce the response of the MIPS device with commercial strain gages, mounted in the same position as the MIPS transducer, were quite successful for times greater than approximately 0.5 msec as shown in Fig. 11. Figure 11 shows oscilloscope traces of the change in voltage across the gage due to the strain. The strain gate circuit is shown in Fig. 12; contact between the marble and glass triggers the oscilloscope trace. Commercial gages gave no

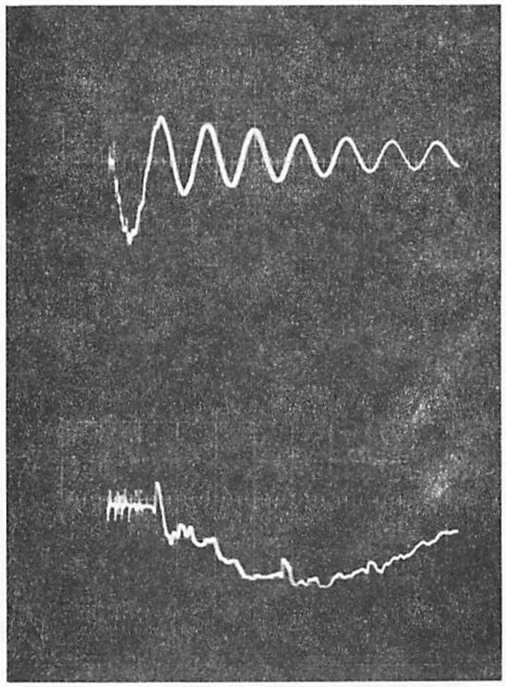

amplification ≈ 6,000
vertical 0.1 V/div
horizontal 5.0 ms/div (top)
0.5 ms/div (bottom)

Fig. 11. Response of wire strain gage mounted on impact-loaded cantilevered beam.

response for time less than approximately 75 μsec after impact possibly because of a poor bond between the gate and the glass. (Various types of cement were employed—SR-4 cement, Armstrong strain gage cement, and Eastman 910.) The strain gages used for Fig. 11 were SR-4 type FAP-12-12S-6 gages with a resistance of 120 ohms and a gage factor of 2. It should be noted that an amplification of approximately 6,000 by a 140 kHz bandwidth AD-YU Type 108-A transistor amplifier was necessary in order to bring the strain gage output voltage to the level of the MIPS transducer output.

The implications of the last two paragraphs have led to the conclusion that the surface strain versus time curves given by the oscilloscope traces of Fig. 9 are very likely a true representation of the beam response. The results shown in Fig. 9 were found to be repeatable on several CdS MIPS devices, provided the location of the device was the same. Figures 9b and 9d show typical reproducibility found for a particular mounting and device. The shape of the response was found to be independent of the quiescent operating point as expected, provided that the source-to-drain voltage was sufficient to keep the MIPS transistor operating in the pinch-off region.

B. Static Response of CdSe MIPS Transducers

Further evaluation of the MIPS theory was made by using CdSe MIPS transducers to measure static strains.

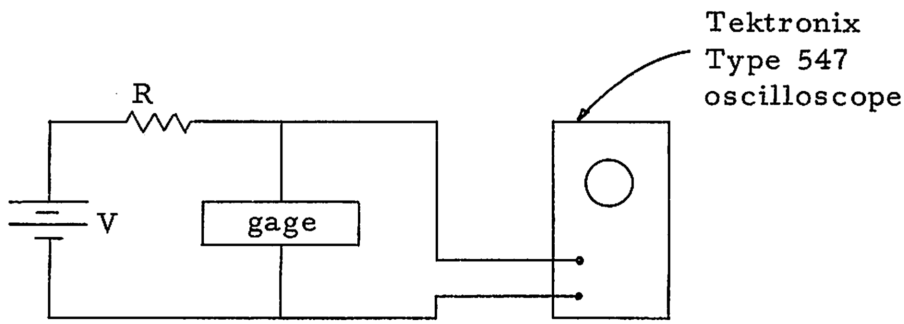

R = 40, 000 Ω

V = 300 V

Gage SR-4 Type FAP-12-12S-6

Gage Resistance = 120 Ω

Gage Factor = 2

Fig. 12. Strain gage biasing and detection circuit.

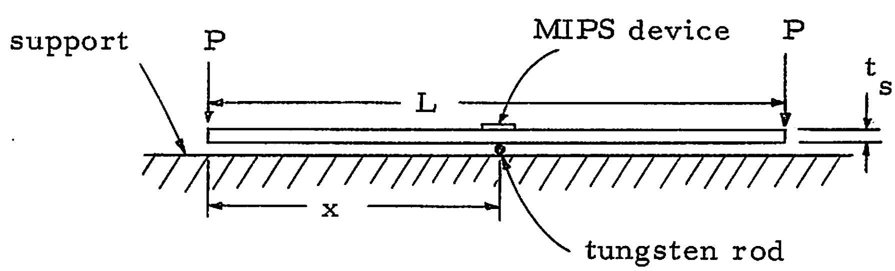

Fig. 13. Mounting used to produce known strain in MIPS transducers.

The method used to strain the CdSe MIPS devices is the same as that used by Muller and Conragan[1] and is illustrated in Fig. 13. A tungsten rod is placed under the MIPS transducer to be tested, and the ends of the substrate are bent until contact is made with the supporting surface. In this way, reproducible strains can be applied. The data used to determine the surface strain $S_s(x)$ were obtained using the circuit of Fig. 3.

For strains applied in the manner shown in Fig. 13 with $x = L/z$ applied surface strain is given by[1]

$$S_s = 6t_s\, d/L^2 , \qquad (22)$$

where t_s = thickness of the substrate,

d = maximum deflection of the neutral axis,

L = length of the substrate as indicated in Fig. 13.

The results obtained from stressing three typical vacuum deposited CdSe MIPS devices made from Harshaw "random cutting" crystalline material are shown in Table 1. The information contained in the table is for MIPS transducers that have been strained as shown in Fig. 13. The values of Applied Strain listed were calculated using Eq. 22 and the appropriate values of t_s, d, and L for the mounting of the particular device. The measured strain values

TABLE I

Strain Data for CdSe MIPS Transducers

	MIPS No. 1	MIPS No. 2	MIPS No. 3
L(in.)	2 5/16	2	2 1/4
d(in.)	0.010	0.010	0.010
t_s(in.)	0.048	0.048	0.048
Applied strain	5.4×10^{-4}	7.2×10^{-4}	5.7×10^{-4}
C'_g(pf)	382	355	334
$g_m R_1$	27.8	25.0	40.0
ΔV_{ds}(V)	0.425	0.500	0.650
V_d(V)	3.0	3.0	3.0
Measured strain	5.9×10^{-4}	7.1×10^{-4}	5.4×10^{-4}

were obtained from Eq. 14 using the data of Table 1. The value of $g_m R_l$ was found by varying V_g by 0.1 V about the quiescent operating point and applying Eq. 15. The ΔV_{ds} values were measured on a Hewlett-Packard Type 130-C oscilloscope and $R_l = 10.65\ K\Omega$ for all measurements. The agreement between applied and measured strain is then seen to be within ± 10% for all cases.

V. TRANSDUCERS ON FLEXIBLE SUBSTRATES

The benefits of transducer fabrication on flexible substrate are immediately apparent. Thus, attempts were made to locate a flexible material which could withstand the 200° C and 10^{-6} Torr vacuum conditions required for the growth of piezoelectrically-active, semiconducting films. A material which performed well in this role was a polyimide film called Kapton. The adherence and electrical quality observed in this laboratory of the CdS, CdSe, Al and SiO films to this material establish Kapton as a possible substrate material for deposited integrated circuits.

The performance of the transducers evaporated onto Kapton was equivalent to that of devices made on glass substrates. After they were made, it was possible to demonstrate a novel form of microphone.

To construct the microphone, a sheet of Kapton roughly 1 × 3 cm onto which a MIPS transducer has been deposited, was placed in tension by suspending it on a frame and attaching a 100 g weight to its lower edge. Indium-soldered leads permitted biasing of the MIPS transducer into its active mode. The biasing and detection circuit is the same as that shown in Fig. 3. Although the mechanical attachments were relatively crude, it was a simple matter to develop a 10 millivolt signal across a 10 kilohm load when the microphone was activated by a normal speaking voice.

VI. ANOMALOUS BEHAVIOR OF SOME CdSe TRANSDUCERS

Approximately 30 of the MIPS devices, made from Harshaw "radom cutting" crystalline CdSe, were checked for the polarity of the drain current change when the CdSe layer was elongated (i.e., positive strain values) and when the CdSe layer was compressed (i.e., negative strain values). All of the devices exhibited an increase in drain current when positive strains were applied and a decrease in drain current when the applied strain was negative. This observation coincides with the behavior of all CdS MIPS devices checked by Conragan[3] and this author (more than 100 devices have been tested). An increase in drain current in response to positive strain in the CdSe film results from a reduction in V_o as can be seen from Eq. (5). A reduced V_o implies an induced positive surface-charge density. This sign of induced charge corresponds to the insulator-CdSe surface, being composed of Se planes.[1]

Initially it was assumed that the evaporated CdSe films were hexagonal crystallites with the c-axis normal to the substrate. X-ray study had established that this was the case for the CdS films.[1] Under this condition, values for the piezoelectric coefficient of CdSe given by Berlincourt et al.[8] would apply and the reduction of the piezoelectric tensor carried out in the section on MIPS theory is valid.* When the excellent agreement between MIPS and applied strain (Table 1) was obtained it seemed evident that the CdSe, as well as the CdS films, consisted almost exclusively of hexagonal (wurtzite) structure with the c-axis normal to the substrate. Hence, it appeared that the experimental data necessary for this report were complete. However, shortly after the experimental work leading to the results of Table 1 was completed, the supply of Harshaw random cutting crystalline CdSe was exhausted. At this time, the crystalline CdSe source was replaced with Harshaw hard sintered cake CdSe. The SiO oxide source and boat were also replaced at the same time. For these new CdSe MIPS transducers, the drain current decreased for a positive strain and increased for a negative strain, in contrast to the previous results. When more devices were constructed and tested it was found that some, but not all of them, exhibited this anomalous behavior.

---

* The piezoelectric coefficient data of reference 8 is stated to apply to hexagonal single-crystal CdSe; however, the article does not indicate that any X-ray studies of the crystals were made.

A decrease in drain current for a positive strain corresponds to the insulator-CdSe surface plane of the film having more Cd atoms than Se atoms. In order to gain further insight into the cause for the different sign of the induced surface charge, X-ray studies of the two types of CdSe films were made. The results of X-ray analysis of CdSe films deposited from the two different sources are discussed in the appendix.

The results in the appendix indicate that CdSe films from crystalline and sintered cake sources both have approximately the same percentages of hexagonal (35%) and cubic (65%) components. A comparison of the orientation of the two types of CdSe films was not possible since the random cutting crystalline source had been exhausted.

If the CdSe hexagonal phase and cubic phase have their c-axis and [111] direction, respectively, normal to the substrate, it is reasonable to expect the piezoelectric coefficient e_{31} to be approximately the same as that given by Berlincourt et al.[8] Provided that the SiO-CdSe surface plane is essentially all Se atoms. This conclusion is evident from the discussion of the piezoelectric effect earlier in this report. Hence, it appears that because of the excellent agreement of MIPS and applied strain in Sec. IV, the vacuum deposited random crystalline CdSe films tend to be oriented such that the c-axis of the hexagonal phase and the [111] direction of the cubic phase are normal to the substrate surface. It is also apparent that the crystallites forming the CdSe film have Se surface planes.

In terms of the discussion for the polarity of the transducer gain, it is evident that the deposited sintered-cake CdSe films would have a Cd interface adjacent to the insulator. If the difference between the two types of CdSe films is only in the direction of the c-axis of the crystallites, the piezoelectric coefficient e_{31} should have the same magnitude, but opposite sign. This positive e_{31} accounts for the decrease in drain current for positive strains observed on most of the sintered cake source MIPS devices.

To check the value of e_{31}, two sintered cake MIPS devices (i.e., the two devices that were made from the CdSe films used for X-ray orientation studies in the appendix) were d.c. biased and stressed in the manner shown in Fig. 13. Both devices behaved anomalously, that is, drain current decreased for a positive strain. In order to match the value of surface strain found using measured MIPS responses in Eq. (14) to the known applied strain, e_{31} would have to be approximately 0.3 c/m^2 for one transducer and approximately 0.4 c/m^2 for the other. By contrast, the piezoelectric coefficient obtained in the manner described above for the CdSe devices made with "random cutting" source material were found to be in the range $-0.14 \leq e_{31} \leq -0.18\ c/m^2$. The data necessary for the calculations are given in Table 1. The value of e_{31} is $-0.16\ c/m^2$ for single-crystal hexagonal CdSe.[8]

Two possible causes for the different behavior of the MIPS devices made from the sintered source material suggest themselves immediately. First, the relatively large percentage of cubic phase CdSe with the [311] direction normal to the substrate (see appendix part B) may have an appreciable effect on e_{31}, and may also make the reduction of the piezoelectric tensor on page 4 invalid. Second, it is possible that the sintered material results in a mixture of growth directions for the individual crystallites making up the films.

In order to determine the actual cause for the different behavior of the two types of CdSe MIPS devices, a thorough investigation of the oxide-CdSe interface is necessary, as well as further crystallographic studies with X-ray techniques.

VII. CONCLUSIONS

The results of the dynamic studies on MIPS electromechanical transducers are significant because they tend to confirm the prediction[1] that CdS MIPS transducers have a high sensitivity and flat gain to high frequencies. In fact, it is shown that the speed of response of the MIPS transducers to mechanical stress or strain approaches that of the constituent MOS transistor itself (i.e., transconductance cutoff). The results of the ultrasonic drill experiment show that CdS MIPS devices made in this laboratory respond to applied stress with substantially their static sensitivity at a frequency of 20 kHz. Transient response studies of MIPS response to mechanical impact loading are consonant with beam theory. The impact loading data were reproducible in a number of devices and were independent of quiescent operating point as predicted by MIPS theory. Confirmation of the fact that MIPS transducers provide an accurate measure of an applied static strain has been given by Muller and Conragan for CdS MIPS devices.[1] In this report, such confirmation was obtained for transducers which had been fabricated from vacuum deposited, random cutting crystalline CdSe. In conclusion, it is noted that strains on the order of 10^{-3} have been produced in both CdSe and CdS films. Although this value of strain is near the failure point for the glass substrate, there was no indication of fracture in the semiconductor layer. A rupture of the semiconductor layer or of the oxide insulator would be evident by a drastic change in the transistor characteristics.

The MIPS microphone described in Sec. IV is of special interest for a number of reasons. First it represents an application of a MIPS transducer deposited on a completely flexible substrate. With the achievement of deposition on a flexible substrate, one can consider such things as adhesive-backed strain gages which can be conveniently applied to a stressed body. The inherent small size (active strain resolving regions of the order of 0.025 by 1.0 mm are quite feasible), the nearly flat transfer function from dc to some megacycles and the high sensitivity of the MIPS transducer make possible the construction of high performance, miniature microphones. Impedance matching this microphone to an associated amplifier could be easily accomplished by direct deposition of an adjacent source-follower thin-film transistor.

The anomalous behavior of the CdSe devices made of sintered material appears to reside in the differing crystal structure of these films from those made with the "random cutting" CdSe. Further study of these films should be directed to understanding their crystalline nature.

REFERENCES

1. R. S. Muller and J. Conragan, IEEE Trans. on Electron Devices, Vol. E.D.-12, 590 (1965).

2. R. S. Muller and J. Conragan, Appl. Phys. Letters, Vol. 6, 83 (1965).

3. J. Conragan, "Physical effects in metal-insulator-piezoelectric semiconductor transistors," M. S. thesis, University of California, Berkeley (1964).

4. R. S. Muller, J. Conragan and J. Fiebiger, Proc. IEEE, Vol. 54, 337 (1966).

5. M. L. Conragan, "Etch-pattern studies of CdS thin films," Consolidated Quarterly Progress Report No. 14, May 16-August 15. University of California, Electronics Research Laboratory, Berkeley, California (1964).

6. W. G. Cady, Piezoelectricity, McGraw-Hill Book Co., New York, (1946) p. 192.

7. R. D. Middlebrook, Proc. IEEE, Vol. 51, 1146 (1963).

8. D. Berlincourt, H. Jaffe and L. R. Shiozawa, Phys. Rev., Vol. 129, 1004 (1963).

9. H. K. J. Ihantola and J. L. Moll, Solid-State Elect., Vol. 7, 423 (1964).

10. J. R. Hauser, IEEE Trans. on Electron Devices, Vol. E.D.-12, 605 (1965).

11. S. H. Crandall and N. C. Dahl, An Introduction to the Mechanics of Solids, McGraw-Hill Book Co., Inc., New York (1959).

12. K. E. Barnhart, Jr and W. Goldsmith, J. Appl. Physics, Vol. 24, 440 (1957).

13. W. Goldsmith and G. W. Norris, Jr., Proc. of the 3rd U. S. Nat. Congress of Appl. Mech., Providence, R. I., (1958) p. 153.

14. F. V. Shallcross, RCA Review, Vol. 24, 676 (1963).

15. A. R. Von Hippel, Dielectrics and Waves, John Wiley & Sons, Inc., New York (1964) p. 201.

APPENDIX

X-RAY ANALYSIS OF CdSe FILMS

The only vacuum-deposited films made from random cutting, crystalline CdSe films that were available for x-ray studies were embodied in MIPS transducers. Consequently, orientation studies of these films were not possible. Intensity data were obtained from an x-ray study of CdSe powder that had been scraped from one of the crystalline-source MIPS devices. Analysis of the x-ray diffraction pattern indicated that these CdSe films were approximately 35% hexagonal phase and 65% cubic phase. These values are considered to be only accurate to within ± 10% because of experimental errors.

Films made from the sintered-cake CdSe source were analyzed more extensively. Three films of this material were deposited on a glass substrate. One of the films was scraped from the substrate for x-ray analysis using the powder pattern technique to determine the phases present. One of the remaining films was studied with a trace diffractometer, an instrument which indicates film orientation. After these x-ray studies were made, MIPS transducers were constructed with the remaining two films. The resultant devices exhibited anomalous transducing characteristics but were characterized by high values of transconductance and output resistance.

The intensity data from a powder pattern indicated that these deposited, sintered cake CdSe films were approximately 30% hexaagonal phase and 70% cubic phase—a result similar to that observed on the CdSe films made from the random cutting, crystalline CdSe.

The results of the trace diffractometer scannings are summarized in Table A-1 below. The tolerances in Table A-1 are the result of errors in the x-ray analyses, rather than being indicative of variations in phase and orientation between the different CdSe films.

Table A-1

Results of Trace Diffractometer Scannings of Sintered Cake CdSe Films

Phase	Indices	Per cent
Hexagonal	[001]	15 - 35
Hexagonal	[112]	2 - 8
Cubic	[111]	30 - 50
Cubic	[311]	20 - 35
Random		< 10

T = substrate temperature = 140° C

X-ray data reported by F. Shallcross[14] on vacuum-deposited CdSe films made at the RCA Research Laboratory, Princeton, N. J., are given in Table A-2. The films were deposited at RCA using comparable evaporation procedures. Devices made at RCA from these films are similar in behavior to those fabricated here; hence, the films may be presumed to have comparable structure. It is evident that the CdSe films consist mainly of hexagonal-phase crystallites having their c-axes normal to the substrate and cubic-phase crystallites, with the [111] direction normal to the sbustrate. The RCA data are the result of a more thorough x-ray study and, as is evident from the tolerances in Table A-1, are a more reliable estimate for the actual film structure.

Table A-2

RCA X-ray Data of Vacuum Deposited CdSe Films

	$T = 50^{o}C$	$T = 230^{o} C$
% hexagonal [001]	28%	23%
% cubic [111]	56%	71%
% hexagonal [100]	4%	1%
% cubic [311]	2%	1%
% hexagonal [112]	2%	1%
% hexagonal [103]	1%	1%
% other orientations*	7%	2%

T = substrate temperature

* Note: No particular orientation and phase included here constitutes more than 1% of the film.

The x-ray data show that the CdSe films tend to consist more of the cubic zinc blende structure (sphalerite) than of the hexagonal wurtzite structure. The CdS films were shown to be approximately 90% wurtzite and 10% sphalerite.[5] These results are to be expected, for reasons outlined by Von Hippel.[15] The following discussion paraphases the arguments put forth by Von Hippel. Consider the diatomic CdX molecule of Fig. 1 and its tetrahedral array of dipole moments. It is known from organic chemistry that for ethane and similar molecules, the staggered position is the stable configuration because the CH_3 groups in the eclipsed position are in steric (spatial) contact and thus repel each other.[15] In the case of the CdX compounds the contending groups are CdX_3 and XCd_3 of opposite polarity; thus electrostatic attraction favors the eclipsed, and steric hindrance favors the staggered position. The ionicity is less and the size is greater for sulfur than for selenium. Hence CdS, having a greater dipole moment than CdSe, favors the eclipsed position and thus the wurtzite structure. In CdSe films the steric hindrance is dominant, and the staggered configuration of cubic zinc blende structure predominates.

The foregoing x-ray analyses, particularly the results of Table A-2, point out the variation in the crystal structure of deposited CdSe films as deposition parameters are altered. This variation, which has not been observed in deposited CdS films, is thought to underly the anomalous behavior of one class of CdSe transducer. Further study is needed to learn, in detail, the source for the anomaly.